

WILEY

Frontiers in Flow Cytometry™

24 hour Virtual Event

September 13th, 2023

Frontiers in Flow Cytometry™ is for researchers across the globe looking for an opportunity to share and learn about current developments in flow cytometry. This 24 hour virtual event will feature keynote presentations by industry colleagues, webinars, demos, live networking opportunities and more.

Key topics include:

- Spectral and conventional flow cytometry
- Immunophenotyping and Standardization
- Panel design and optimization
- Cancer Biology and Auto-immune Diseases
- Infectious diseases
- Advances in flow cytometry technology

[Register Now](#)

This event is sponsored by **ThermoFisher**
SCIENTIFIC

Correlates of deviance detection in auditory brainstem responses of bats

Johannes Wetekam  | Julio Hechavarría  | Luciana López-Jury  |
Manfred Kössl

Institute of Cell Biology and
Neuroscience, Goethe University,
Frankfurt am Main, Germany

Correspondence

Johannes Wetekam and Manfred Kössl,
Institute of Cell Biology and
Neuroscience, Goethe University, Max-
von-Laue-Str. 13, 60438 Frankfurt am
Main, Germany.
Email: wetekam@bio.uni-frankfurt.de;
koessl@bio.uni-frankfurt.de

Funding information

Deutsche Forschungsgemeinschaft

Edited by: Sophie Molholm

Abstract

Identifying unexpected acoustic inputs, which allows to react appropriately to new situations, is of major importance for animals. Neural deviance detection describes a change of neural response strength to a stimulus solely caused by the stimulus' probability of occurrence. In the present study, we searched for correlates of deviance detection in auditory brainstem responses obtained in anaesthetised bats (*Carollia perspicillata*). In an oddball paradigm, we used two pure tone stimuli that represented the main frequencies used by the animal during echolocation (60 kHz) and communication (20 kHz). For both stimuli, we could demonstrate significant differences of response strength between deviant and standard response in slow and fast components of the auditory brainstem response. The data suggest the presence of correlates of deviance detection in brain stations below the inferior colliculus (IC), at the level of the cochlea nucleus and lateral lemniscus. Additionally, our results suggest that deviance detection is mainly driven by repetition suppression in the echolocation frequency band, while in the communication band, a deviant-related enhancement of the response plays a more important role. This finding suggests a contextual dependence of the mechanisms underlying sub-cortical deviance detection. The present study demonstrates the value of auditory brainstem responses for studying deviance detection and suggests that auditory specialists, such as bats, use different frequency-specific strategies to ensure an appropriate sensation of unexpected sounds.

KEYWORDS

ABR, MMN, prediction error, repetition suppression, SSA

Abbreviations: ABR, Auditory brainstem response; AN, Auditory nerve; ANOVA, Analysis of variance; CN, Cochlear nucleus; DC, direct current; HW, Hardware; IC, Inferior colliculus; MGB, Medial geniculate body; MS, Many-standards; SOC, Superior olivary complex; SSA, Stimulus-specific adaptation; SW, Software.

A Commentary on this Article is available here: <https://doi.org/10.1111/ejn.15606>

This is an open access article under the terms of the Creative Commons Attribution-NonCommercial License, which permits use, distribution and reproduction in any medium, provided the original work is properly cited and is not used for commercial purposes.

© 2021 The Authors. *European Journal of Neuroscience* published by Federation of European Neuroscience Societies and John Wiley & Sons Ltd.

1 | INTRODUCTION

Deviance detection is the ability of the brain to detect unexpected cues and allows animals to react appropriately to an ever-changing environment. A neural mechanism that is likely linked to this ability is stimulus-specific adaptation (SSA), a phenomenon first reported about two decades ago (Ulanovsky et al., 2003). It describes specific changes in the reaction patterns of some neurons in the form of decreased firing rates in response to high probability (standard) sounds and increased firing rates in response to low probability (deviant) sounds. Deviance detection (for a detailed review on this topic; see Carbajal & Malmierca, 2018) has been studied in a variety of different species (e.g. mice: Anderson et al., 2009; rats: Von Der Behrens et al., 2009; cats: Ulanovsky et al., 2004; gerbils: Bäuerle et al., 2011; bats: Thomas et al., 2012; and humans: Näätänen et al., 2007, Näätänen et al., 1978) and has been found in several brain areas, from inferior colliculus (IC) to cortex (Ayala et al., 2015; Bäuerle et al., 2011; Chen et al., 2015; Nieto-Diego & Malmierca, 2016; Tsolaki et al., 2015). It has been suggested that deviance detection is the product of two underlying mechanisms that cooperate to encode the statistical probability of a stimulus through neural response strength. These mechanisms are repetition suppression on the one hand and response enhancement caused by unexpected stimuli (referred to as prediction error or ‘genuine’ deviance detection) on the other hand. In a recent paper, Duque et al. (2018) used auditory brainstem response (ABR) recordings to study deviance detection in subcortical brain structures of the mouse and while they did not find evidence for deviance detection in the typical fast waves of the ABR, they unveiled an IC-related slow wave following the fast ones, called p_0 , that was significantly larger for deviant sounds compared with standard sounds (Duque et al., 2018). Although many questions remain, the results from Duque et al. (2018) opened the gate for studying deviance detection using minimally invasive ABRs.

The present study has several goals that build upon but are different from those addressed in previous work:

1. We were interested in knowing whether slow ABR waves that are sensitive to deviance detection, like those described in rodents, also occur in another group of mammals with even more sophisticated auditory perception, namely bats. To that end, ABRs were recorded in anaesthetized bats (*Carollia perspicillata*) while the animals listened to mixtures of standard and deviant sounds. Our results confirmed the existence of a slow wave sensitive to deviance detection in the ABR of bats. Our data also revealed that these slow waves might not be related to IC activity only, as

previously thought, but may be influenced as well by activity in auditory centres below the IC in the auditory hierarchy. In addition, we also report deviance detection in some of the fast waves (ii–iv) which were previously not known to be influenced by stimulus probability.

2. We aimed to assess whether the putative mechanisms underlying deviance detection—that is, repetition suppression and prediction error—are visible in ABR waves. To investigate this, besides testing the classic oddball paradigm, we included data from the so-called many-standards paradigm (Carbajal & Malmierca, 2018; Parras et al., 2017; Schröger & Wolff, 1996). The data suggest that the proportional contribution of the underlying deviance detection mechanisms differs between the echolocation (60 kHz) and communication (20 kHz) frequency band.

2 | MATERIALS AND METHODS

2.1 | Animals

For this study, 20 specimens of the bat species *C. perspicillata* (15 females, 5 males), weighting between 16 and 23 g, were used. Animals were caught from the university’s breeding colony and were held in a separate cage during the course of the study. For all experiments, animals were initially anaesthetised by a subcutaneous injection of a mixture of ketamine (Ketavet © 10%, Medistar GmbH Ascheberg, Germany; 0.5 mg per 100 g bodyweight) and xylazine (Rompun © 2%, Bayer HealthCare AG, Mohnheim, Germany; 2 mg per 100 g bodyweight) and in some of the experiments a second injection of the same solution was performed after 60 min, with 70% of the initial volume. This resulted in recording sessions lasting between 90 and 180 min. The body temperature of 37°C was maintained by a direct current (DC) powered heating pad attached to the animal holder, and two consecutive recording sessions in the same animal were separated by at least 5 days. All experiments of this study were performed in compliance with current German laws and were approved by the Regierungspräsidium Darmstadt (permits: FR/1010; FU/Anz. 1002).

2.2 | Stimulation and recording procedure

For sound generation and signal recording, custom written MATLAB® scripts (MathWorks Inc., USA) were used. The digital stimuli were D/A-converted by a 192-kHz Fireface UC soundcard (RME, Haimhausen, Germany),

fed into a custom made HiFi amplifier and presented to the animal through a Fountek Neo X3.0 ribbon tweeter (I.T. Intertechnik GmbH, Kerpen, Germany) at a distance of 15 cm from the animal's left ear. During the recording, the animal's head was fixed in a mouth-holder to ensure that the speaker was pointing optimally towards the left ear with a constant 45° azimuth angle between loudspeaker and head. All stimuli were pure tone pulses of 10-ms duration with rise-fall times of 1 ms and amplitudes of 60-dB SPL. The sound repetition rate was 20 Hz unless otherwise stated. To elicit deviance detection, an oddball paradigm was used, containing two stimuli of different frequencies—A and B—that were presented in a pseudo random order with different probabilities of appearance. In a first sequence, stimulus A was presented as standard (90%, 900 repetitions) and stimulus B as deviant (10%, 100 repetitions) and in a second sequence their roles were switched. To further investigate the properties of the observed deviance detection, several control experiments were performed. In the so-called many-standards control (Schröger & Wolff, 1996), the standard stimulus was replaced by nine different pure tones spanning a frequency range between 20 and 80 kHz, all of which had the same probability of occurrence as the deviant (10%). In this way, the response to the target tone was unaffected by both repetition suppression and prediction error effects and thus could be used as a baseline control to study the influence of both components on the deviant and standard responses. In a second control, the frequency gap between the stimulus and the accompanying tone of the oddball sequence was logarithmically reduced to determine the minimum frequency-distance between both sounds to elicit deviance detection. Lastly, in a subsample of animals, the classic oddball paradigm was repeated with a reduced stimulus repetition rate of 8 Hz.

ABRs were recorded by two insulated silver wires (AG-10T, diameter: 0.25 mm; uninsulated and chlorinated tip of 3 mm), placed subcutaneously along the midline of the animal's skull and next to the bulla of the left middle ear, respectively. A ground electrode was treated with conductive cream and clipped to the contralateral thumb. The recorded responses were amplified 20 k-fold and band-pass filtered between 0.1 and 3000 Hz (20 dB/decade roll-offs) by a Dagan EX1 differential amplifier (Science Products GmbH, Hofheim, Germany). Subsequently, blocks of 20 consecutive points of the input signal were averaged, resulting in a downsampling rate of 9.6 kHz.

2.3 | Data processing

The recorded ABRs were saved and offline processed in MATLAB®. To assess different frequency components

of the ABR, the signals were filtered in two different ways, with a broad (10–3000 Hz) and a narrow (300–3000 Hz) band-pass Butterworth filter (fourth order). While the broadband filter provided an almost unchanged 'raw' ABR that contained all slow and fast components of the response, the narrowband filter allowed a more precise evaluation of the fast waves in the signal. For the averaging procedure, only deviant responses following a standard response were used. To ensure a similar signal-to-noise ratio between standard and deviant averages, standard responses must have been followed by a deviant response to be included in the average. This resulted in an equal number of deviant and standard responses (between 84 and 94 trials) used to calculate the average responses of a given individual. Additionally, by this procedure, effects of repetition suppression on the analysed standard responses were maximised. The same criterion was used to determine the responses of the many-standards condition; however, since the pseudo random order of the many-standards sequence was different from that of the oddball sequence, slightly different numbers of trials might have been used to calculate the average (mean difference: 1.2 trials). Baseline correction of each individual average was performed by calculating the mean voltage of the filtered signal during a time window of 1 ms just before stimulus onset and subtracting this value from the whole signal, that is, normalising the average pre-stimulus activity to 0 µV. As a measure of response strength, the RMS of the recorded signals was calculated within defined temporal windows and compared between conditions. For the broadband filtered signal, only one window was set to cover the whole raw ABR with all its components (slow and fast waves) which started 0.5 ms and ended 13 ms after stimulus onset for responses to either stimulus. This is in accordance with the temporal interval used by a former publication to study ABRs in *C. perspicillata* (Wetekam et al., 2020). On the other hand, for the narrowband filtered signals, three windows were applied that covered one fast wave each. With respect to slightly different peak latencies of the 60- and 20-kHz responses, the borders of the individual windows had to be adapted accordingly. The following values (post-stimulus onset) were used for responses to 60-kHz tones: 0.5–1.8 ms (wave i), 1.8–2.9 ms (waves ii/iii) and 2.9–4.1 ms (wave iv). For responses to 20-kHz tone pips, the following temporal windows were applied: 0.5–2.1 ms (wave i), 2.1–3.1 ms (waves ii/iii) and 3.2–4.3 ms. These latencies of the fast waves i–iv are similar to those of previous ABR studies in other bat species (*Eptesicus fuscus*: Burkard & Moss, 1994; *Phyllostomus discolor*: Hörpel & Firzlaff, 2020; Linnenschmidt & Wiegrebe, 2018).

2.4 | Statistical evaluation

Based on the parametric structure of the RMS data—which was confirmed by Kolmogorov–Smirnov tests—paired one-tailed *t*-tests and repeated measure analyses of variance (ANOVAs) with subsequent Bonferroni-corrected post-hoc tests were used to evaluate statistical differences in the response strength between different conditions (standard, deviant, control). To evaluate the size of the measured effect, Cohen's *D* was calculated for each significant comparison. According to Cohen (1988), values between 0.2 and 0.5 are referred to as small effect size, values from 0.5 to 0.8 as medium effect size and values > 0.8 as large effect size.

3 | RESULTS

C. perspicillata uses echolocation as its main sense for orientation and, due to the highly social lifestyle of this animal; it has developed a rich repertoire of communication calls (Knörnschild et al., 2014). Echolocation and communication occupy different frequency bands of the bat's vocal repertoire with dominant peak frequencies around 60 and 20 kHz, respectively (Figure 1; Hechavarría et al., 2016; Martin et al., 2017). To investigate potential differences between both frequency bands, we recorded ABRs to two different pure tone stimuli, presented as standards and deviants: 60- and 20-kHz pure tones.

3.1 | Characterisation of the recorded ABRs

When considering the shape of the broadband filtered ABRs, the typical fast ABR waves were always superimposed by a larger positive slow wave, lasting up to ~13-ms post-stimulus onset. Amplitude and duration of this slow wave were dependent on the stimulus

frequency, with higher amplitudes and longer durations in responses elicited by the 20-kHz pure tones, when compared with the 60-kHz stimulus (Figure 2a,c; upper panels). Onset and peak latency of the slow wave were 1- to 1.5-ms and 5- to 6-ms post-stimulus onset, respectively. When the narrowband filter was applied, the slow component entirely disappeared from the signal, leaving behind the typical ABR waves i to iv, similar in shape to those reported by other studies in bats (e.g. *P. discolor*: Hörpel & Firzlaß, 2020; Linnenschmidt & Wiegrebe, 2018; *E. fuscus*: Burkard & Moss, 1994). Waves ii and iii merged into one, sometimes double-peaked wave which was treated as one unit in this study. As opposed to the slow component of the broadband filtered signal, amplitude and duration of the waves i–iv did not depend as strongly on the stimulus frequency. Remarkably, wave i was double peaked in the responses to the 20 kHz but not to the 60-kHz stimulus (Figure 2a,c; lower panel).

3.2 | Deviance detection in ABRs

ABRs were recorded in an oddball paradigm to investigate correlates of deviance detection in the auditory pathway. Additionally, a many-standards control was included to disentangle the underlying neural mechanisms that contribute to the measured effect. Considering the broadband filtered signal, response strength was significantly smaller when the 60-kHz stimulus was presented as a standard as compared with when the same stimulus was presented as a deviant or in the many-standards control sequence (ANOVA: $F = 5.75$, $p = 7.0 * 10^{-3}$; standard-deviant: $p = 0.011$, standard-control: $p = 0.047$; Figure 2b, left). This indicates a significant effect of repetition suppression in the raw ABR signal. The same applies to wave ii/iii (ANOVA: $F = 7.19$, $p = 2.5 * 10^{-3}$; standard-deviant: $p = 7.2 * 10^{-3}$, standard-control: $p = 0.012$) and wave iv (ANOVA: $F = 20.01$, $p = 1.81 * 10^{-6}$; standard-deviant:

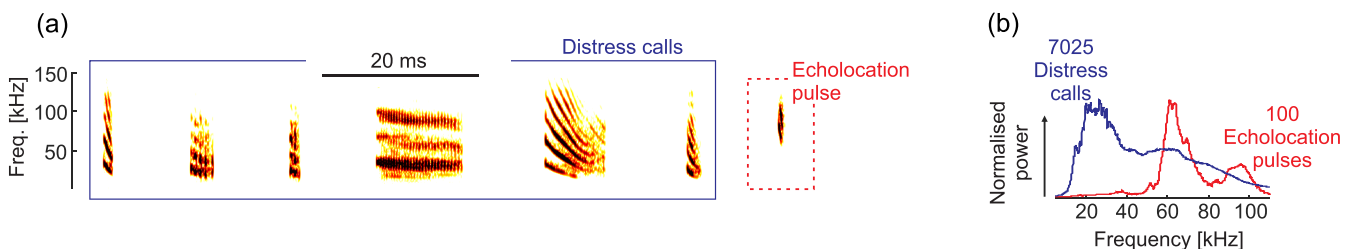


FIGURE 1 Frequency spectra of communication and echolocation vocalisations of *Carollia perspicillata*. (a) Spectrograms of example distress (i.e. communication) and echolocation vocalisations. (b) Median normalised power spectra of distress and echolocation vocalisations with peaks around 20 and 60 kHz, respectively

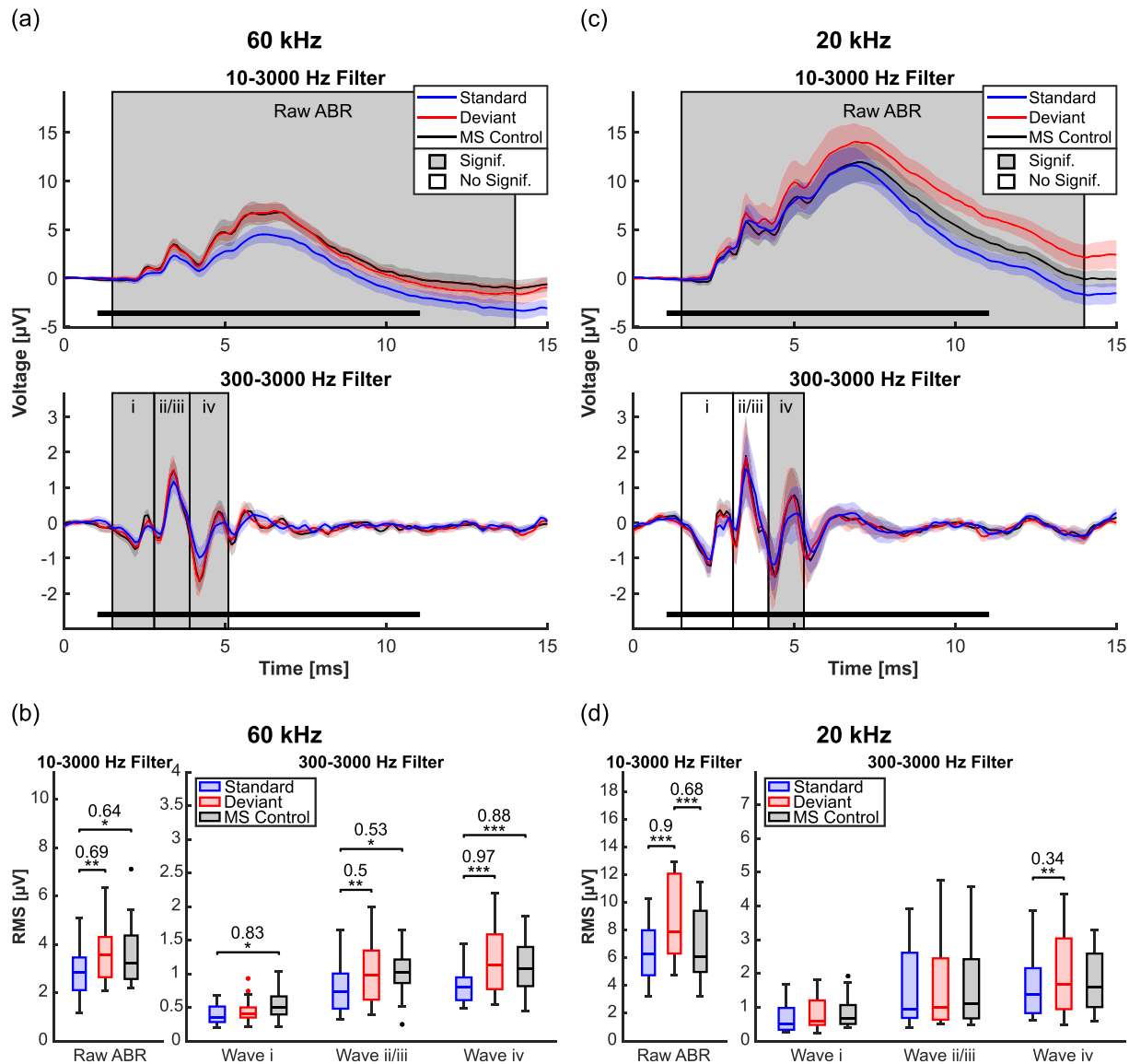


FIGURE 2 Deviance detection in broadband and narrowband filtered auditory brainstem responses (ABRs). (a) Grand averages of broadband (10–3000 Hz, upper panel) and narrowband (300–3000 Hz, lower panel) filtered ABRs to a 60-kHz pure tone stimulus, presented as standard and deviant as well as in the many-standards (MS) control sequence ($n = 18$ animals). The boxes depict the time windows taken for RMS calculation, containing the whole raw ABR of the broadband filtered signal as well as wave i, wave ii/iii and wave iv of the narrowband filtered signal, respectively. If at least one corrected post-hoc comparison of response strength between the different conditions provided a significant difference, the respective time window is shaded in grey; otherwise, it is transparent. The shaded area around the graphs depicts the standard error of the mean, and stimulus duration is indicated by a black bar at the bottom left. (b) Boxplots of the RMS values calculated for each of the 18 individual-responses within the time windows, both for the broadband filtered raw ABR (left) and the narrowband filtered waves i–iv (right). Asterisks indicate significant differences between groups and as a measure of effect size; Cohen's D is plotted as a number above the asterisks every time significance was reached. (c, d) As in panels (a) and (b) but the stimulus was a 20-kHz pure tone

$p = 2.8 * 10^{-4}$, standard-control: $p = 7.0 * 10^{-4}$) of the narrowband filtered signal but not to wave i where the standard was significantly reduced compared with the control but not in comparison with the deviant (ANOVA: $F = 5.23$, $p = 0.011$; standard-control: $p = 0.020$; Figure 2b, right). When the stimulus was a 20-kHz pure tone, the deviant response was significantly larger than

the standard and control response (ANOVA: $F = 17.75$, $p = 5.26 * 10^{-6}$; standard-deviant: $p = 8.7 * 10^{-4}$, deviant-control: $p = 1.3 * 10^{-4}$; Figure 2d, left). This is evidence for the presence of a prediction error component that is driving deviance detection in the 20-kHz band. In the narrowband filtered signal, a significantly increased deviant response was only obtained for wave iv

(ANOVA: $F = 6.05$, $p = 5.7 * 10^{-3}$; standard-deviant: $p = 7.5 * 10^{-3}$; Figure 2d, right). Note, however, that while the effect size was either medium or large for all other significant differences, it was small for the last comparison (Figure 2d, wave iv).

Additionally, to be able to better evaluate the influence of the slow component on the observed effects in the broadband filtered signal, another comparison of response strength was performed with RMS values derived from the same responses, but low-pass filtered (10–300 Hz), leaving behind only the slow waves. The significant differences were the same as for the broadband filtered raw ABRs (60 kHz: ANOVA: $F = 6.34$, $p = 4.6 * 10^{-3}$; standard-deviant: $p = 6.7 * 10^{-3}$, standard-control: $p = 0.022$; 20 kHz: ANOVA: $F = 18.34$, $p = 3.95 * 10^{-5}$; standard-deviant: $p = 7.4 * 10^{-4}$, deviant-control: $p = 7.7 * 10^{-4}$), and all effect sizes were slightly increased when the fast components were filtered out (Figure 3). This finding demonstrates the importance of the slow wave for deviance detection in the raw ABR.

3.3 | Influence of stimulus frequency-distance and repetition rate

To further characterise the phenomena observed, we gradually reduced the frequency difference between deviant and standard stimulus in a logarithmic manner to identify the minimal distance between the two oddball stimuli that was required to elicit a significant difference in response strength. For this experiment, a subset of 10 animals was used and only the broadband filtered responses were taken into consideration, as they showed the strongest effects of deviance detection (Figures 2 and 3). For the 60-kHz stimulus, deviant and standard responses were significantly different when the accompanying pure tone had frequencies of 20 kHz ($t = 2.67$, $p = 0.026$), 40 kHz ($t = 5.85$, $p = 2.4 * 10^{-4}$) or 50 kHz ($t = 2.62$, $p = 0.028$), with medium to large effect sizes (0.58–1.25). Narrower frequency-distances of 5, 2.5 and 0 kHz did not produce significant differences; hence, the minimal spectral gap between both tones required to elicit deviance detection was 10 kHz (Figure 4a,c). For the 20-kHz tone, however, only the largest tested distance of 40 kHz (i.e. an accompanying oddball stimulus of 60 kHz) evoked significant deviance detection ($t = 2.43$, $p = 0.038$) with a medium effect size (Figure 4b,d). In summary, these results demonstrate stimulus-specific differences in the frequency resolution of deviance detection, with higher resolutions in the 60-kHz band.

To ensure a better comparability with other studies in the field, where lower stimulus repetition rates were applied (e.g. Duque et al., 2018; Grimm et al., 2011;

Malmierca et al., 2009; Slabu et al., 2010; Ulanovsky et al., 2003), we used another subset of 10 animals to record deviance detection with a reduced stimulus presentation rate of 8 Hz and compared the results to the responses of the same animals evoked by the 20-Hz repetition rate. While the change of repetition rate had no obvious effect on the 60-kHz raw ABRs (20 Hz: $t = 2.67$, $p = 0.026$; 8 Hz: $t = 4.52$, $p = 1.5 * 10^{-3}$; Figure 5a,b), it did affect the 20-kHz responses. The significant difference between deviant and standard response in the temporal window of the broadband filtered signal between 0.5 and 13 ms that was present when the repetition rate was 20 Hz ($t = 2.43$, $p = 0.038$) disappeared when the sound presentation rate was reduced to 8 Hz. However, a second window, following the first one and lasting from 13- to 24-ms post-stimulus onset now revealed significant deviance detection with a large effect size ($t = 3.12$, $p = 0.012$; Figure 5c,d). This contrasts the three other conditions (60-kHz stimulus, repetition rate of 20 and 8 Hz; 20-kHz stimulus, repetition rate of 20 Hz) where no significant deviance detection could be unveiled in the later window. Thus, the repetition rate influenced the time point of the first appearance of deviance detection in the signal but only under certain stimulation circumstances. Moreover, the experiment revealed a general increment of response strength after the stimulation rate was reduced, independent of the stimulus frequency and probability (Figure 5, supporting information Figure S1). This, however, is most likely related to unspecific adaptation effects in the lower auditory system and not to deviance detection per se.

4 | DISCUSSION

The general aim of this study was to investigate deviance detection in ABRs of a hearing specialised mammal. In this context, we characterised the obtained responses with respect to their dependence on stimulus frequency and repetition rate. We could demonstrate that (1) Significant effects of deviance detection are present in the slow and fast components of the ABR and are measurable at earlier time points than previously known—already at wave ii/iii, before IC onset. (2) The contribution of repetition suppression and prediction error to deviance detection in broadband filtered ABRs differs in a stimulus-dependent manner. Repetition suppression is dominant in the 60-kHz (echolocation) frequency band, while deviance detection is driven by a prediction error component in the 20-kHz (communication) band. (3) The frequency resolution of deviance detection is different between both tested frequency bands. (4) Reducing the stimulus repetition rate can delay the first appearance of deviance

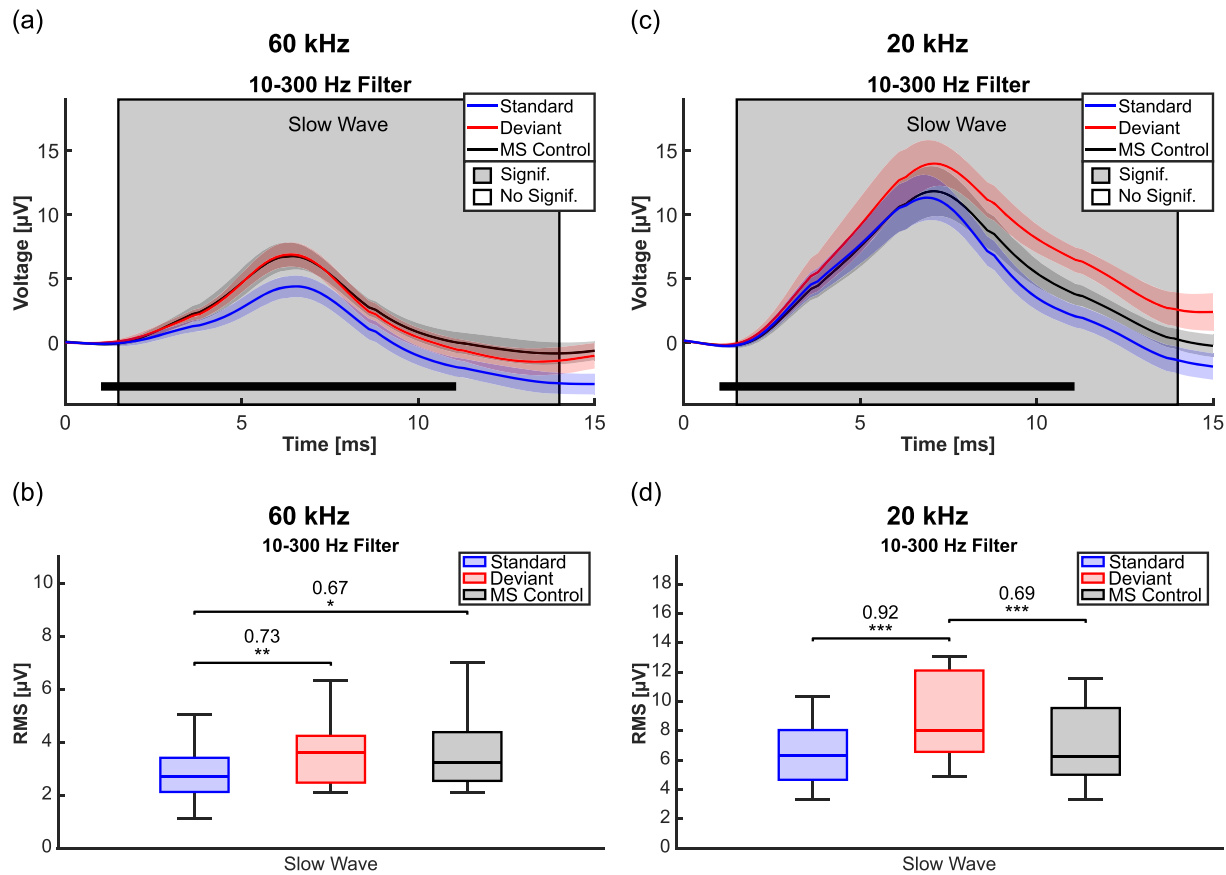


FIGURE 3 Deviance detection in the isolated slow wave of the auditory brainstem response (ABR). (a) Grand averages of low-pass filtered (10–300 Hz) ABRs to a 60-kHz pure tone stimulus, presented as standard and deviant as well as in the many-standards (MS) control sequence ($n = 18$ animals). The boxes depict the time windows taken for RMS calculation, containing the isolated slow wave component of the ABR. If at least one comparison of response strength between the different conditions provided a significant difference, the respective time window is shaded in grey; otherwise, it is transparent. The shaded area around the graphs depicts the standard error of the mean and stimulus duration is indicated by a black bar at the bottom left. (b) Boxplots of the RMS values calculated for each of the 18 individual-responses within the time window shown in (a). Asterisks indicate significant differences between groups and as a measure of effect size; Cohen's D is plotted as a number above the asterisks every time significance was reached. (c, d) As in panels (a) and (b) but the stimulus was a 20-kHz pure tone

detection in ABRs but does not erase it. In summary, the results demonstrate the value of minimally invasive ABR recordings for investigations of deviance detection in the lowest stations of the auditory pathway and highlight a stimulus specificity of deviance detection, measurable in the bat brain.

4.1 | Neural correlates of the ABR slow wave

When broadband filtered, the ABRs recorded for this study were dominated by a positive low frequency component with onset latencies between 1 and 1.5 ms and lasting until up to ~ 13 -ms post-stimulus onset. Despite the fact that most ABR studies so far focus on narrow-band filtered responses that usually do not contain slow

components, similar waves were also reported in a few previous studies for both humans and animals (Barry & Barry, 1996; Battmer & Lehnhardt, 1981; Duque et al., 2018; Land et al., 2016). The neural origin of this slow wave, often referred to as p_0 , has been suggested to lie in the IC and to represent an early sustained response of it (Barry & Barry, 1996; Land et al., 2016). However, a pure IC-origin of the slow wave, as suggested by Land et al., 2016, is questionable in our case due to the very early onset latencies of the slow wave. Potentially, the slow component rather reflects a summation of neural activity of several auditory nuclei, the earliest of which might lie in peripheral areas (brainstem) but with the IC as its main contributor, responsible for the peak amplitude and peak latency. An artificial broadening of the slow wave caused by data filtering could be ruled out using an artificial stimulus that was fed into the

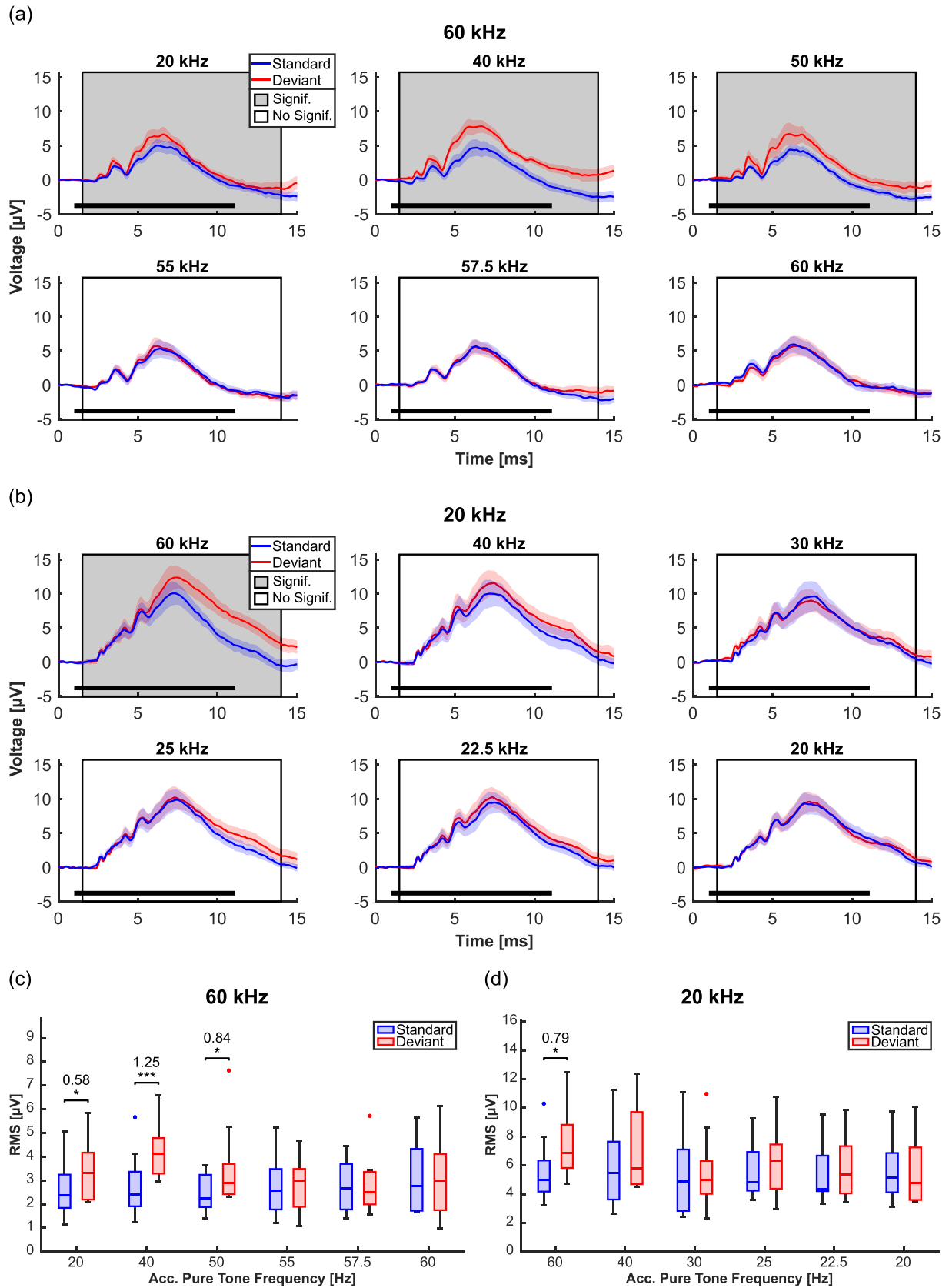


FIGURE 4 Legend on next page.

FIGURE 4 Dependence of deviance detection on the frequency difference between deviant and standard stimulus. (a) Grand averages of broadband filtered (10–3000 Hz) auditory brainstem responses (ABRs) to a 60-kHz pure tone stimulus, presented as standard and deviant, respectively ($n = 10$ animals). Given on top of each panel is the frequency of the accompanying pure tone which was presented together with the stimulus in the oddball paradigm (20 to 60 kHz). The boxes depict the time windows taken for RMS calculation, containing the raw ABR. If the comparison of response strength between deviant and standard provided a significant difference, the respective time window is shaded in grey; otherwise, it is transparent. The shaded area around the graphs depicts the standard error of the mean and stimulus duration is indicated by a black bar at the bottom left. (b) As in (a) but the stimulus was a 20-kHz tone, and the accompanying pure tones went from 60 to 20 kHz. (c) Boxplots of the RMS values calculated for each of the 10 individual-responses within the time window shown in (a). Asterisks indicate significant differences between groups and as a measure of effect size; Cohen's D is plotted as a number above the asterisks every time significance was reached. (d) As in (c) but the stimulus was a 20-kHz pure tone, and the accompanying pure tones went from 60 to 20 kHz

hardware filter (supporting information Figure S2). The input closely resembled the recorded ABRs but had a 2-ms delayed and slightly shorter slow wave component, simulating a sharper peak of IC activity. Neither duration nor onset latency of the slow wave was affected by the filtering, suggesting that the shape and onset latencies of the recorded ABRs solely correlate to neuronal activity. In conclusion, our results demonstrate that the slow ABR wave is a complex yet valuable component that might contain more activity of pre-IC auditory centres than previously thought.

4.2 | Interpretation of the reported deviance detection

Significant RMS differences between standard and deviant response were present in the broadband filtered raw ABRs evoked by either of the two stimuli tested. Low-pass filtering of the same responses revealed that the major effect was driven by the slow component superimposed on the typical fast ABR waves which is likely to be primarily related to IC activity. This is supporting evidence for what was shown in ABRs of mice by Duque et al., 2018, who also demonstrated deviance detection in a similar, IC-related slow wave (p_0). However, as opposed to the study by Duque et al. (2018), we could also show correlates of deviance detection in some of the fast ABR components. Both peaks, wave ii/iii and wave iv of the 60-kHz responses showed significantly larger deviant than standard responses, as did wave iv of the 20-kHz responses. In some animals, this effect was measurable even in wave i (supporting information Figure S1, $n = 10$ animals); however, it was not significant on population level when considering all tested animals (Figure 2, $n = 18$ animals). According to previous work that aimed to identify the neural sources of the fast peaks, wave i represents neural activity in the auditory nerve (AN), waves ii and iii are related to evoked potentials of the cochlear nucleus (CN) and superior olivary complex (SOC), respectively, and wave iv is dominated by IC

activity (Henry, 1979; Land et al., 2016). Note, however, that these studies refer to data obtained in mice, but it can be assumed that the neural ABR generators do not differ significantly between most species, given the similar structure and organisation of the brainstem. In another study in which a bat (*Pteronotus parnellii*) was used as animal model, Hattori and Suga (1997) reported minimum IC latencies around 4 ms. Taken together, this suggests that deviance detection in wave iv (with latencies between 2.9 and 4.3 ms) could be related to IC activity but that the measured differences between standard and deviant response in wave ii/iii (with latencies no longer than 3.1 ms) might indicate deviance detection effects appearing earlier than the first IC onset. Additionally, as described in Section 4.1, brain stations below the IC might also be involved in the generation of deviance detection observed in the slow wave of the raw ABR. To the best of our knowledge, the contribution of brain stations below the IC in the generation of deviance detection responses has not been reported before. However, the phenomena described here could be species specific, given the fact that SSA exhibiting neurons could not be found in the CN of the rat (Ayala et al., 2012) and that several studies that investigated deviance detection in the fast ABR waves of mice and humans could not demonstrate significant effects before (Althen et al., 2011; Duque et al., 2018; Slabu et al., 2010). The fact that bats rely more on their auditory sense than most other mammals and that recognising unexpected acoustic cues is crucial for both echolocation and communication, given the highly social lifestyle of the animals, could play an important role here. The natural stimuli bats are exposed to are often highly repetitive with fast repetition rates (e.g. Simmons, 1989) which might require a more prominent involvement of the brainstem in all aspects of auditory processing, given that high repetition rates are better represented in peripheral compared with higher-order auditory stations (Joris et al., 2004). In a study from 2012, Thomas and colleagues demonstrated the presence of SSA in non-specialised but not in echolocation-specialised neurons in the IC of a bat (species: *E. fuscus*).

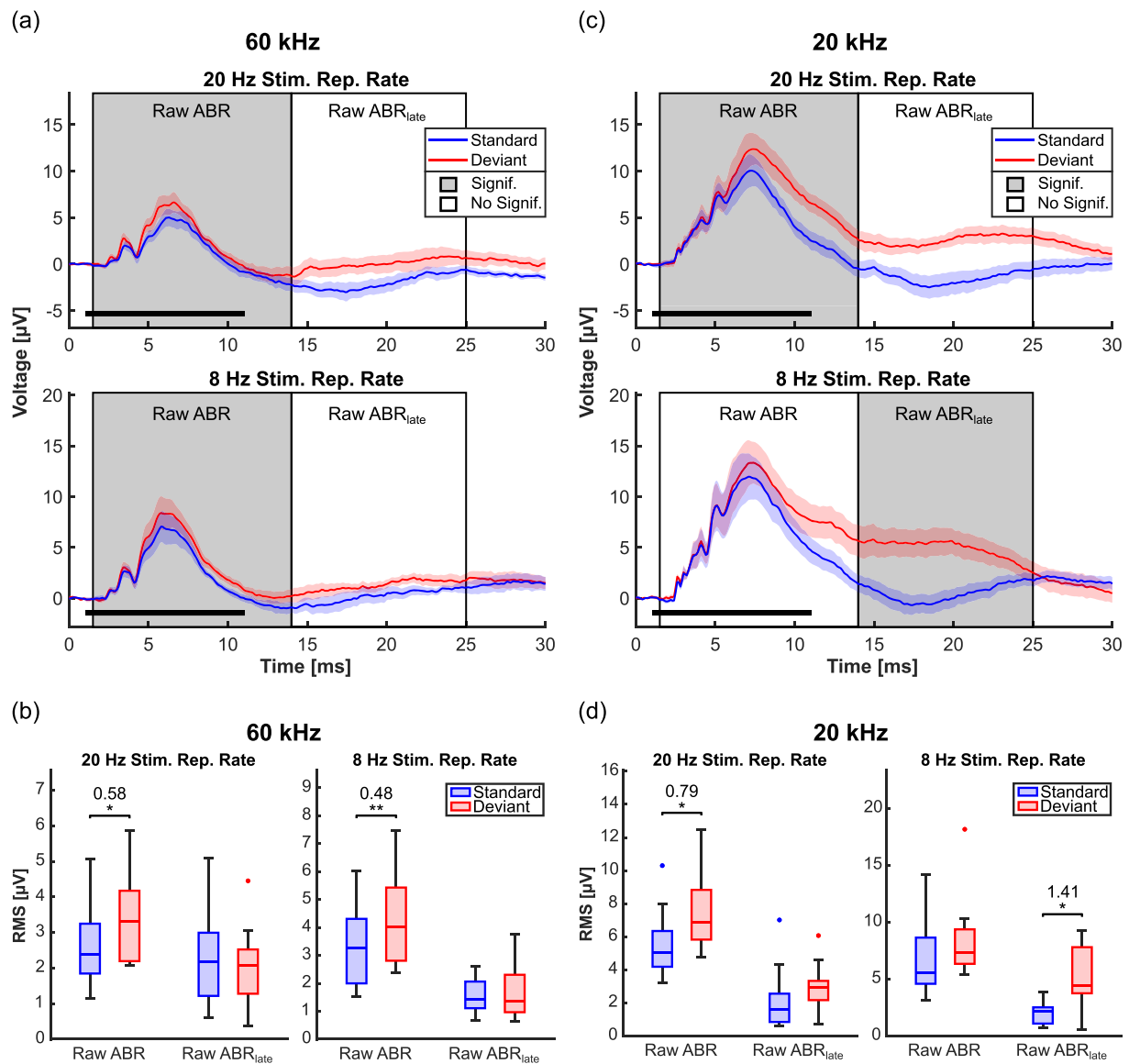


FIGURE 5 Influence of the sound presentation rate on deviance detection in broadband filtered auditory brainstem responses (ABRs). (a) Grand averages of broadband (10–3000 Hz) filtered ABRs to a 60-kHz pure tone stimulus, presented as standard and deviant, respectively ($n = 10$ animals). The sound presentation rate was either 20 Hz (upper panel) or 8 Hz (lower panel). The boxes depict the time windows taken for RMS calculation, containing the raw ABR and the subsequent late raw ABR (raw ABR_{late}), respectively. If the comparison of response strength between deviant and standard provided a significant difference, the respective time window is shaded in grey; otherwise, it is transparent. The shaded area around the graphs depicts the standard error of the mean and stimulus duration is indicated by a black bar at the bottom left. (b) Boxplots of the RMS values calculated for each of the 10 individual-responses within the time windows, both for the raw ABR and the raw ABR_{late}. The sound presentation rate was either 20 Hz (left) or 8 Hz (right). Asterisks indicate significant differences between groups and as a measure of effect size; Cohen's *D* is plotted as a number above the asterisks every time significance was reached. (c, d) As in panels (a) and (b) but the stimulus was a 20-kHz pure tone

The fact that our data yet provide evidence for deviance detection in the echolocation frequency band can be explained by two hypotheses: (1) ABRs might be mainly generated by activity of non-specialised neurons, independent of the stimulus' frequency band. (2) *E. fuscus* is an insect-hunting bat, relying on high-duty cycle echolocation, while *C. perspicillata* is a fruit-eating species with a less specialised echolocation system. Hence, it is likely

that the IC of *C. perspicillata* contains more non-specialised neurons than that of *E. fuscus*, causing prominent deviance detection also in the echolocation frequency band.

A potential mechanism driving deviance detection in brain structures below the IC is descending feedback loops, reaching the most peripheral structures either directly (CN and SOC) or indirectly through the IC

(cochlea and AN; Terreros & Delano, 2015). Although previous studies have shown that efferent cortical projections rather play a modulatory role and are not solely responsible for SSA in the IC (Anderson & Malmierca, 2013) and medial geniculate body (MGB) (Antunes & Malmierca, 2011), their influence on deviance detection in more peripheral auditory stations is unknown.

4.3 | Stimulus-dependent differences

It had been proposed that deviance detection is the product of two different mechanisms which together create the measurable response difference encoding the stimulus probability. These mechanisms are repetition suppression and prediction error and as a means to disentangle both correlates, several control experiments have been suggested in the past (Carbajal & Malmierca, 2018; Parras et al., 2017; Schröger & Wolff, 1996). They are based on the idea of evoking responses that are not influenced by either repetition suppression or prediction error. One of these controls, the so-called many-standards sequence, was used in this study and revealed interesting stimulus-dependent effects in the broadband filtered raw ABR. As for the 60-kHz responses, significant RMS differences between standard and deviant as well as standard and control response suggest a dominant repetition suppression effect. On the other hand, in the 20-kHz responses, significant differences were present between standard and deviant as well as deviant and control response which indicate a more important role of prediction error than repetition suppression. Since 60 and 20 kHz represent the spectral domains of echolocation and communication, respectively, the contrary involvement of the two driving mechanisms might indicate that deviance detection can be influenced by behavioural context. As opposed to the raw ABRs, deviance detection in the fast waves seem to be primarily driven by repetition suppression, independent of the stimuli used. Although the effect did not always reach a significant level, in all the investigated fast waves, a reduction of the standard response was more prominent than an enhancement of the deviant response (Figure 2), indicating that the prediction error component first emerges in the IC.

4.4 | Further classification of deviance detection in the ABR

With two additional control experiments, we aimed to further investigate the dependence of the measured

deviance detection on the stimulus frequency and repetition rate. The first of these experiments revealed that the smallest required frequency-distance between the two tones of the oddball paradigm is different for both tested stimuli but generally high compared with previous single-unit SSA studies (cat: Ulanovsky et al., 2003; rat: Antunes et al., 2010; Malmierca et al., 2009). This higher Δf required to elicit deviance detection in the ABR can be explained by the hypothesis of a minimum number of neurons necessary to evoke a measurable effect in the extracranially recorded sum potentials which is only reached by a comparatively high Δf .

Since most other studies investigating deviance detection used sound presentation rates at or below 10 Hz (e.g. Duque et al., 2018; Grimm et al., 2011; Malmierca et al., 2009; Slabu et al., 2010; Ulanovsky et al., 2003), we recorded another set of data with a reduced stimulus repetition rate of 8 Hz to ensure a better comparability of our data. Neither slow nor fast components of the 60-kHz responses were influenced by the reduced repetition rate when compared with the responses of the same individuals, recorded with the 20-Hz sound presentation rate (Figure 5, supporting information Figure S1). However, for the 20-kHz responses, the temporal shift of deviance detection to a later segment in the broadband filtered signal when the stimulus repetition rate was low, indicates that a higher repetition rate leads to a stronger participation of lower order brain structures and vice versa.

4.5 | Conclusion

In summary, the present study demonstrates that minimally invasive ABR recordings provide an excellent tool to study deviance detection and its underlying mechanisms in the auditory system. Additionally, the data provide reason to reconsider the hypothesis of the IC as the lowest auditory centre involved in deviance detection-generation. The latter requires additional studies that clarify whether the findings reported here can be validated on single-unit level (SSA). Future studies will also be needed to tackle the question whether and to which extend the results of the current study can be applied to other species, including humans.

ACKNOWLEDGEMENT

This study was funded by the Deutsche Forschungsgemeinschaft (KO 987/14-1).

CONFLICT OF INTEREST

The authors declare no conflicts of interests.

AUTHOR CONTRIBUTIONS

Study design: Johannes Wetekam, Julio Hechavarría, Luciana López-Jury and Manfred Kössl. Experiments, analysis and original draft of the manuscript: Johannes Wetekam. Review and editing of the original draft: Julio Hechavarría, Luciana López-Jury and Manfred Kössl.

PEER REVIEW

The peer review history for this article is available at <https://publons.com/publon/10.1111/ejn.15527>.


DATA AVAILABILITY STATEMENT

The data that support the findings of this study are available from the corresponding author upon reasonable request.

ORCID

Johannes Wetekam  <https://orcid.org/0000-0003-1919-3140>

Julio Hechavarría  <https://orcid.org/0000-0001-9277-2339>

Luciana López-Jury  <https://orcid.org/0000-0002-9384-2586>

REFERENCES

- Althen, H., Grimm, S., & Escera, C. (2011). Fast detection of unexpected sound intensity decrements as revealed by human evoked potentials. *PLoS ONE*, *6*(12), e28522. <https://doi.org/10.1371/journal.pone.0028522>
- Anderson, L. A., & Malmierca, M. S. (2013). The effect of auditory cortex deactivation on stimulus-specific adaptation in the inferior colliculus of the rat. *European Journal of Neuroscience*, *37*(1), 52–62. <https://doi.org/10.1111/ejn.12018>
- Anderson, L. A., Christianson, G. B., & Linden, J. F. (2009). Stimulus-specific adaptation occurs in the auditory thalamus. *Journal of Neuroscience*, *29*(22), 7359–7363. <https://doi.org/10.1523/JNEUROSCI.0793-09.2009>
- Antunes, F. M., & Malmierca, M. S. (2011). Effect of auditory cortex deactivation on stimulus-specific adaptation in the medial geniculate body. *Journal of Neuroscience*, *31*(47), 17306–17316. <https://doi.org/10.1523/JNEUROSCI.1915-11.2011>
- Antunes, F. M., Nelken, I., Covey, E., & Malmierca, M. S. (2010). Stimulus-specific adaptation in the auditory thalamus of the anesthetized rat. *PLoS ONE*, *5*(11), e14071. <https://doi.org/10.1371/journal.pone.0014071>
- Ayala, Y. A., Pérez-González, D., Duque, D., Nelken, I., & Malmierca, M. S. (2012). Frequency discrimination and stimulus deviance in the inferior colliculus and cochlear nucleus. *Frontiers in Neural Circuits*, *6*(DEC), 1–19. <https://doi.org/10.3389/fncir.2012.00119>
- Ayala, Y. A., Udeh, A., Dutta, K., Bishop, D., Malmierca, M. S., & Oliver, D. L. (2015). Differences in the strength of cortical and brainstem inputs to SSA and non-SSA neurons in the inferior colliculus. *Scientific Reports*, *5*(January), 1–17. <https://doi.org/10.1038/srep10383>
- Barry, S. J., & Barry, E. K. (1996). ABR slow wave and stimulus duration. *Journal of the American Academy of Audiology*, *7*(1), 7–14.
- Battmer, R. D., & Lehnhardt, E. (1981). The brain stem response SN10, its frequency selectivity, and its value in classifying neural hearing lesions. *Archives of Oto-Rhino-Laryngology*, *230*(1), 37–47. <https://doi.org/10.1007/BF00665378>
- Bäuerle, P., von der Behrens, W., Kössl, M., & Gaese, B. H. (2011). Stimulus-specific adaptation in the gerbil primary auditory thalamus is the result of a fast frequency-specific habituation and is regulated by the corticofugal system. *Journal of Neuroscience*, *31*(26), 9708–9722. <https://doi.org/10.1523/JNEUROSCI.5814-10.2011>
- Burkard, R., & Moss, C. F. (1994). The brain-stem auditory-evoked response in the big brown bat (*Eptesicus fuscus*) to clicks and frequency-modulated sweeps. *Journal of the Acoustical Society of America*, *96*(2), 801–810. <https://doi.org/10.1121/1.410318>
- Carbajal, G. V., & Malmierca, M. S. (2018). The neuronal basis of predictive coding along the auditory pathway: From the subcortical roots to cortical deviance detection. *Trends in Hearing*, *22*, 1–33. <https://doi.org/10.1177/2331216518784822>
- Chen, I. W., Helmchen, F., & Lütcke, H. (2015). Specific early and late oddball-evoked responses in excitatory and inhibitory neurons of mouse auditory cortex. *Journal of Neuroscience*, *35*(36), 12560–12573. <https://doi.org/10.1523/JNEUROSCI.2240-15.2015>
- Cohen, J. (1988). Statistical power analysis for the behavioral sciences. In *Statistical Power Analysis for the Behavioral Sciences* (2nd ed.). Hillsdale, NJ: Lawrence Erlbaum Associates. <https://doi.org/10.4324/9780203771587>
- Duque, D., Pais, R., & Malmierca, M. S. (2018). Stimulus-specific adaptation in the anesthetized mouse revealed by brainstem auditory evoked potentials. *Hearing Research*, *370*, 294–301. <https://doi.org/10.1016/j.heares.2018.08.011>
- Grimm, S., Escera, C., Slabu, L., & Costa-Faidella, J. (2011). Electrophysiological evidence for the hierarchical organization of auditory change detection in the human brain. *Psychophysiology*, *48*(3), 377–384. <https://doi.org/10.1111/j.1469-8986.2010.01073.x>
- Hattori, T., & Suga, N. (1997). The inferior colliculus of the mustached bat has the frequency-vs-latency coordinates. *Journal of Comparative Physiology - A Sensory, Neural, and Behavioral Physiology*, *180*(3), 271–284. <https://doi.org/10.1007/s003590050047>
- Hechavarría, J. C., Beetz, M. J., Macias, S., & Kössl, M. (2016). Distress vocalization sequences broadcasted by bats carry redundant information. *Journal of Comparative Physiology. A, Neuroethology, Sensory, Neural, and Behavioral Physiology*, *202*(7), 503–515. <https://doi.org/10.1007/s00359-016-1099-7>
- Henry, K. R. (1979). Auditory brainstem volume-conducted responses: Origins in the laboratory mouse. *Journal of the American Auditory Society*, *4*(5), 173–178.
- Hörpel, S. G., & Firzlaff, U. (2020). Post-natal development of the envelope following response to amplitude modulated sounds in the bat *Phyllostomus discolor*. *Hearing Research*, *388*, 107904. <https://doi.org/10.1016/j.heares.2020.107904>
- Joris, P. X., Schreiner, C. E., & Rees, A. (2004). Neural processing of amplitude-modulated sounds. *Physiological Reviews*, *84*(2),

- 541–577). American Physiological Society. <https://doi.org/10.1152/physrev.00029.2003>
- Knörnschild, M., Feifel, M., & Kalko, E. K. V. (2014). Male courtship displays and vocal communication in the polygynous bat *Carollia perspicillata*. *Behaviour*, *151*(6), 781–798. <https://doi.org/10.1163/1568539X-00003171>
- Land, R., Burghard, A., & Kral, A. (2016). The contribution of inferior colliculus activity to the auditory brainstem response (ABR) in mice. *Hearing Research*, *341*, 109–118. <https://doi.org/10.1016/j.heares.2016.08.008>
- Linnenschmidt, M., & Wiegrebe, L. (2018). Ontogeny of auditory brainstem responses in the bat, *Phyllostomus discolor*. *Hearing Research*, *373*, 85–95. <https://doi.org/10.1016/j.heares.2018.12.010>
- Malmierca, M. S., Cristaudo, S., Pérez-González, D., & Covey, E. (2009). Stimulus-specific adaptation in the inferior colliculus of the anesthetized rat. *Journal of Neuroscience*, *29*(17), 5483–5493. <https://doi.org/10.1523/JNEUROSCI.4153-08.2009>
- Martin, L. M., García-Rosales, F., Beetz, M. J., & Hechavarría, J. C. (2017). Processing of temporally patterned sounds in the auditory cortex of Seba's short-tailed bat. *European Journal of Neuroscience*, *46*(8), 2365–2379. <https://doi.org/10.1111/ejn.13702>
- Näätänen, R., Gaillard, A. W. K., & Mäntysalo, S. (1978). Early selective-attention effect on evoked potential reinterpreted. *Acta Psychologica*, *42*(4), 313–329. [https://doi.org/10.1016/0001-6918\(78\)90006-9](https://doi.org/10.1016/0001-6918(78)90006-9)
- Näätänen, R., Paavilainen, P., Rinne, T., & Alho, K. (2007). The mismatch negativity (MMN) in basic research of central auditory processing: A review. *Clinical Neurophysiology*, *118*(12), 2544–2590. <https://doi.org/10.1016/j.clinph.2007.04.026>
- Nieto-Diego, J., & Malmierca, M. S. (2016). Topographic distribution of stimulus-specific adaptation across auditory cortical fields in the anesthetized rat. *PLoS Biology*, *14*(3), 1–30. <https://doi.org/10.1371/journal.pbio.1002397>
- Parras, G. G., Nieto-Diego, J., Carbajal, G. V., Valdés-Baizabal, C., Escera, C., & Malmierca, M. S. (2017). Neurons along the auditory pathway exhibit a hierarchical organization of prediction error. *Nature Communications*, *8*(1), 2148. <https://doi.org/10.1038/s41467-017-02038-6>
- Schröger, E., & Wolff, C. (1996). Mismatch response of the human brain to changes in sound location. *NeuroReport*, *7*(18), 3005–3008. <https://doi.org/10.1097/00001756-199611250-00041>
- Simmons, J. A. (1989). A view of the world through the bat's ear: The formation of acoustic images in echolocation. *Cognition*, *33*(1–2), 155–199. [https://doi.org/10.1016/0010-0277\(89\)90009-7](https://doi.org/10.1016/0010-0277(89)90009-7)
- Slabu, L., Escera, C., Grimm, S., & Costa-Faidella, J. (2010). Early change detection in humans as revealed by auditory brainstem and middle-latency evoked potentials. *European Journal of Neuroscience*, *32*(5), 859–865. <https://doi.org/10.1111/j.1460-9568.2010.07324.x>
- Terreros, G., & Delano, P. H. (2015). Corticofugal modulation of peripheral auditory responses. *Frontiers in Systems Neuroscience*, *9*(September), 1–8. <https://doi.org/10.3389/fnsys.2015.00134>
- Thomas, J. M., Morse, C., Kishline, L., O'Brien-Lambert, A., Simonton, A., Miller, K. E., & Covey, E. (2012). Stimulus-specific adaptation in specialized neurons in the inferior colliculus of the big brown bat, *Eptesicus fuscus*. *Hearing Research*, *291*(1–2), 34–40. <https://doi.org/10.1016/j.heares.2012.06.004>
- Tsolaki, A., Kosmidou, V., Hadjileontiadis, L., Kompatsiaris, I., & Tsolaki, M. (2015). Brain source localization of MMN, P300 and N400: Aging and gender differences. *Brain Research*, *1603*, 32–49. <https://doi.org/10.1016/j.brainres.2014.10.004>
- Ulanovsky, N., Las, L., Farkas, D., & Nelken, I. (2004). Multiple time scales of adaptation in auditory cortex neurons. *Journal of Neuroscience*, *24*(46), 10440–10453. <https://doi.org/10.1523/JNEUROSCI.1905-04.2004>
- Ulanovsky, N., Las, L., & Nelken, I. (2003). Processing of low-probability sounds by cortical neurons. *Nature Neuroscience*, *6*(4), 391–398. <https://doi.org/10.1038/nn1032>
- Von Der Behrens, W., Bäuerle, P., Kössl, M., & Gaese, B. H. (2009). Correlating stimulus-specific adaptation of cortical neurons and local field potentials in the awake rat. *Journal of Neuroscience*, *29*(44), 13837–13849. <https://doi.org/10.1523/JNEUROSCI.3475-09.2009>
- Wetekam, J., Reissig, C., Hechavarría, J. C., & Kössl, M. (2020). Auditory brainstem responses in the bat *Carollia perspicillata*: Threshold calculation and relation to audiograms based on otoacoustic emission measurement. *Journal of Comparative Physiology. A, Neuroethology, Sensory, Neural, and Behavioral Physiology*, *206*(1), 95–101. <https://doi.org/10.1007/s00359-019-01394-6>

SUPPORTING INFORMATION

Additional supporting information may be found in the online version of the article at the publisher's website.

How to cite this article: Wetekam, J., Hechavarría, J., López-Jury, L., & Kössl, M. (2022). Correlates of deviance detection in auditory brainstem responses of bats. *European Journal of Neuroscience*, *55*(6), 1601–1613. <https://doi.org/10.1111/ejn.15527>